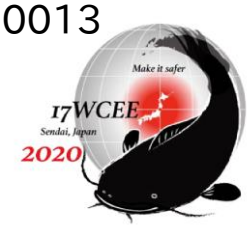

17th World Conference on Earthquake Engineering, 17WCEE

Sendai, Japan - September 13th to 18th 2020

EXPERIMENTAL BEHAVIOR OF TWO REHABILITATED BEAM-COLUMN CONNECTIONS UNDER CYCLIC LOADING

H. Guerrero[(1)], V. Rodríguez[(2)], S.M. Alcocer[(3)], J.A. Escobar[(4)], R. Gomez[(5)], E. Tapia[(6)]

[(1)] *PhD Student, Institute of Engineering, UNAM, Mexico, vrodriguezmo@iingen.unam.mx*
[(2)] *Associate Professor, Institute of Engineering, UNAM, Mexico, hguerrerob@iingen.unam.mx*
[(3)] *Research Professor, Institute of Engineering, UNAM, Mexico, salcocerm@iingen.unam.mx*
[(4)] *Research Professor, Institute of Engineering, UNAM, Mexico, jess@pumas.iingen.unam.mx*
[(5)] *Research Professor, Institute of Engineering, UNAM, Mexico, rgomezm@iingen.unam.mx*
[(6)] *Research Professor, Institute of Engineering, UNAM, Mexico, etapiah@azc.uam.mx*
…

Abstract

After the 2017 Mexico earthquakes, significant efforts have been devoted to improve the seismic performance of damaged structures. In that context, two beam-column connections have been tested at full scale under cyclic loading. During the experiments, a displacement-controlled protocol was applied at the tip of the beam by means of a hydraulic actuator. Cross-sectional areas were 600x600 mm for the columns and 450x810 mm for the beams. The specimens were tested up to severe damage (with concrete spalling and crushing and evidence of elongation of longitudinal reinforcement, but not buckling nor fracture). Rehabilitation was carried out using two different techniques. Externally bonded carbon fiber reinforced polymer was used for one specimen and jacketing with high-strength steel-fiber reinforced mortar was used for the other. Re-testing of the specimens was conducted in order to assess the adequacy of the rehabilitation procedures. The results showed that both specimens were able to recover their load-carrying and deformation capacities. As a consequence, comparisons between the original and rehabilitated specimens were conducted and are presented in this paper in terms of visible damage and cracking. Other parameters like strength and drift capacity are compared as well. Conclusions, useful for the rehabilitation of concrete connections damaged during earthquakes, are offered.

Keywords: Beam-column connections; cyclic loading; experimental test; seismic rehabilitation

1. Introduction

After the September 19, 2017 Mexico earthquakes, which caused significant structural damage in the States of Morelos, Puebla and parts of Mexico City, substantial efforts have been devoted to the development of seismic protection technologies for new structures, and of rehabilitation methods that improve the seismic performance of existing damaged structures. Traditional repair and strengthening techniques of reinforced concrete structures include partial or total replacement of concrete, concrete or steel jacketing, external post-tensioning, epoxy repair, etc. [1]. Many of these techniques are labor-intensive, invasive and, in many cases, difficult to implement. In this study, two reinforced concrete (RC) monolithic beam-column connections were rehabilitated with techniques that were considered practical in terms of application. One of the specimens was repaired with externally bonded carbon fiber reinforced polymer (CFRP) sheets, while the other was repaired with a high-strength steel fiber reinforced mortar (SFRM). In this paper, the abbreviation SFRM will be used when referring to a mixture without coarse aggregate.

CFRP materials are an option to traditional techniques. They are lightweight, reasonably easy to install, non-corroding, and have shown to have excellent fatigue characteristics and high strength in the fiber direction [2, 3]. Additional advantages include low labor cost, limited disruption to building occupancy, no significant increase in member sizes, and require less maintenance than traditional techniques [1]. Studies conducted by Bonfiglioli et al. [4] and Shahawy et al. [5] have demonstrated that CFRP materials are a viable option for repair, rehabilitation and strengthening of RC members as well as increasing their fatigue life. Flexural, shear and torsional strengthening can be achieved with different sheet wrap configurations. For example, Ghobarah et al. [6] found that the torsional strength of concrete beams can be upgraded significantly by completely wrapping the torsion zone rather than having discontinuities in the CFRP sheets.

Recently, the use of steel-fiber reinforced concrete (SFRC) has increased due to its many structural uses such as for industrial slabs, pavements, concrete toppings, precast structures, shell type structures, and structural repairing [7]. Advantages of using SFRC include increase in tenacity in flexion; increase of tension, shear, and torsion strength; increase of impact and fatigue resistance; improvement of contraction and creep behavior; and increased durability in certain weather conditions [8]. Due to the versatility and advantages of SFRC, many areas of opportunity, have been identified. Carrillo et al. [9] studied the use of SFRC for low-rise housing since brittle failure in beams, columns and walls can be avoided. Ávila et al. [10] implemented the rehabilitation of structural concrete walls with SFRC after being severely damaged due to seismic actions.

In Mexico, interest in using CFRP, SFRM and SFRC for numerous structural practices has grown significantly, particularly in the National Autonomous University of Mexico, where studies have been recently conducted and continue to be carried out.

2. Experimental Program

Two full-scale exterior monolithic RC beam-column connections were tested under quasi-static cyclic loading. After testing, each specimen was rehabilitated using a different technique, namely: 1) wrapping with carbon fiber reinforced polymer; and 2) casing with steel-fiber reinforced mortar. Only beams were rehabilitated.

Beams were oriented vertically while columns laid horizontally and were connected to the reaction slab by means of post-tensioned steel bars (see Fig. 1). This allowed limited rotation restraints to the columns to simulate their stiffness. A displacement-controlled loading protocol was applied at the beam's tip with a hydraulic actuator.

2.1 Test specimens

Specimens C-1 and C-2 were exterior RC beam-column connections with beam and column lengths of 5 and 3.3 m, respectively. Their cross-sections were 450x810 mm and 600x600 mm, respectively. Specimen

geometry and detailing are shown in Fig. 2. Labels and general characteristics of the original and rehabilitated specimens are summarized in Table 1. It is worth highlighting that both specimens were intentionally designed to have large stirrup spacing (300 mm) in order to comply with low ductility requirements according to the Mexico City Building Code [11]. Further, specimens were designed to develop a strong column-weak beam mechanism.

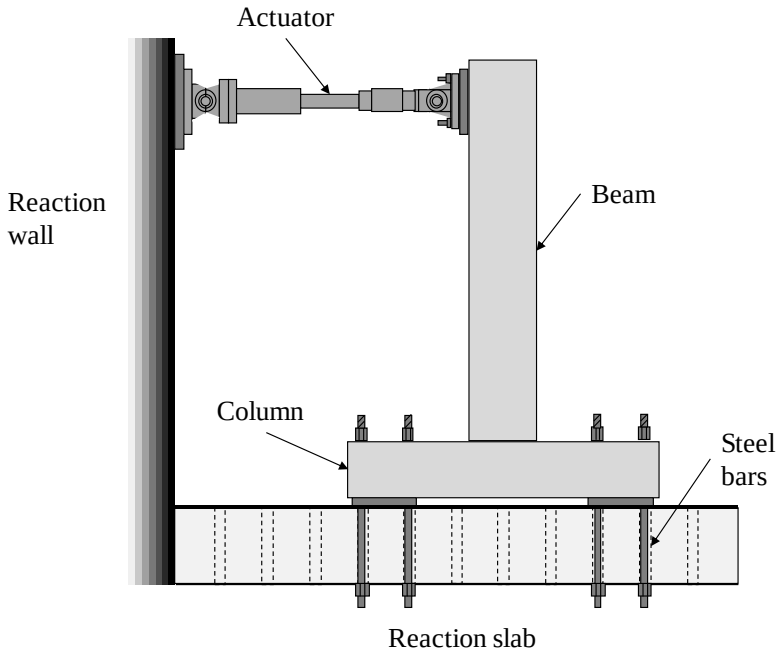

Fig. 1 – Experiment setup

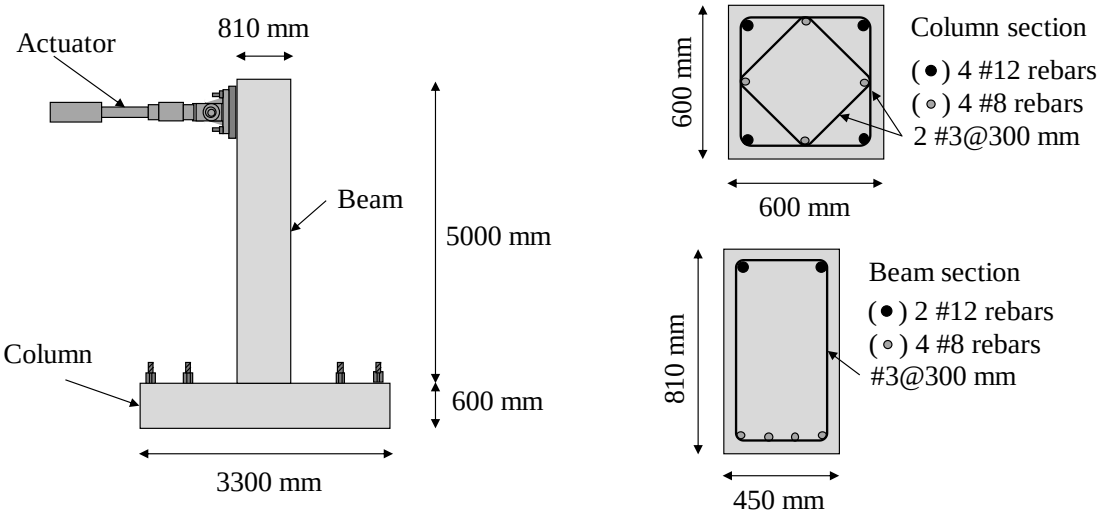

Fig. 2 – Specimen geometry and detailing

Materials used in the original specimens were concrete with an average compression strength of 55 MPa (measured from cylinder samples), and steel bars with a nominal yielding strength of 420 MPa. Rehabilitation of specimen C-1 was carried out with CFRP sheets, which consisted of Sikadur ® 300 polymer and Sikawrap ® 530 carbon fiber (which had a nominal thickness of 1.3 mm, an elastic modulus of 240,000 MPa, and an ultimate tension strength of 4,000 MPa). The SFRM used for the rehabilitation of specimen C-2 had an average compressive strength of 85.5 MPa at 28 days (measured from sampled cubes).

Table 1 – Characteristics of tested specimens

Specimen	Attribute	Rebar percentage		Stirrups
		Top	Bottom	
C-1	Monolithic	0.69%	0.62%	#3@300 mm
C-1/CFRP	Repaired with CFRP			
C-2	Monolithic			
C-2/SFRM	Repaired with SFRM			

2.2 Instrumentation

Local deformations and displacements were assessed by means of linear variable differential transducers (LVDTs). Horizontal LVDTs were placed along the beam to measure displacements; vertical LVDTs were placed to measure rotations; and diagonal LVDTs were located on the side faces of the beam and joint in order to assess shear deformations (see Fig. 3).

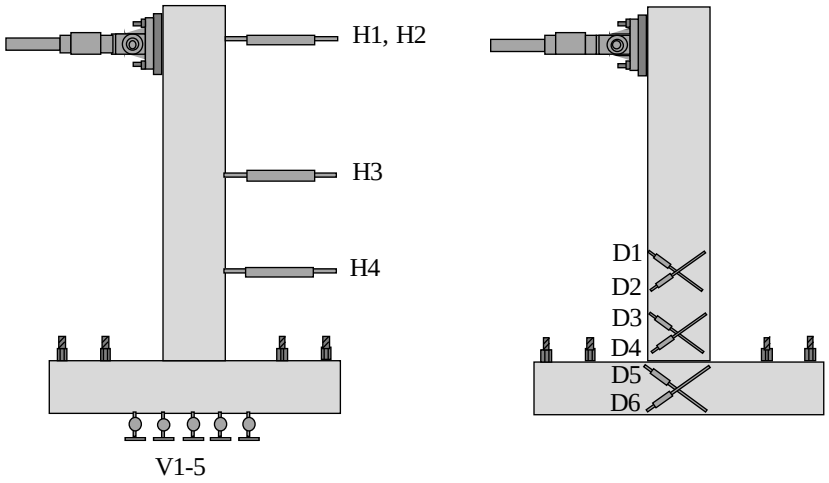

Fig. 3 – Instrumentation of specimens

2.3 Loading protocol

Two different loading protocols were used for the tests in order to evaluate the response of the beam-column connections to various load cycles. These protocols, shown in Fig. 4, follow recommendations given by ACI 374.2R-13 [12]. The displacement history shown in Fig. 4a was applied to specimens C-1 and C-1/CFRP and consisted of two cycles for each displacement target, followed by a smaller cycle at 50% the displacement reached in the previous cycle. Specimens C-2 and C-2/SFRM were tested with the loading protocol shown in Fig. 4b. In this case three cycles were applied for each displacement target, followed by a smaller cycle as with specimen C-1. Additionally, more displacement targets were incorporated.

Effects resulting from the use of different loading protocols are discussed in Section 4. Failure of specimens was considered when the lateral resistance was below 80% of the peak strength or when specimens had lost stability and could put instruments or personnel at risk.

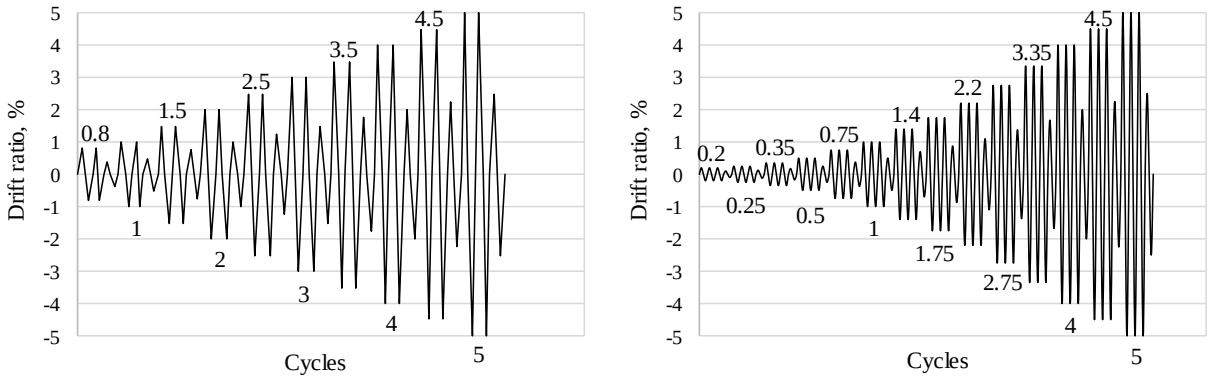

a) Protocol for specimen C-1 and C-1/CFRP b) Protocol for specimens C-2 and C-2/SFRM

Fig. 4 – Loading protocols of specimens

3. Rehabilitation Process

As mentioned above, the performance of two rehabilitation techniques was evaluated. Specimen C-1 was repaired with CFRP sheets and specimen C-2 was repaired with SFRM. In both cases, only the beam hinge region was repaired. A brief description of both rehabilitation process is provided below.

3.1 Specimen C-1/CFRP

The rehabilitation process of specimen C-1 began with cleaning of the concrete surface, followed by the injection of epoxy in cracks less than 2-mm wide. Voids and cavities were filled with a high-strength mortar with a compressive strength of 70 MPa. Finally, the CFRP sheets were placed after applying a coat of resin. The criteria used for the wrapping of the beam was to confine the plastic hinge region of the beam. Confinement was provided with one layer in the longitudinal direction and one in the transverse direction with lengths of 1.6 and 1.1 m, respectively. Two more sheets were added to the column in order to secure the longitudinal sheets of the beam. Fig. 5a shows the final state of specimen C-1/CFRP.

a) C-1/CFRP b) C-2/SFRM

Fig. 5 – Repaired specimens

3.2 Specimen C-2/SFRM

Specimen C-2 was rehabilitated with a 40 mm thick jacket of high-strength SFRM (see Fig. 5b). The process started with a cleaning of the surface. Cracks were filled with mortar and an adhesive material was placed on the concrete surface in order to bond the SFRM with the existing concrete. Formwork and SFRM were

placed and covered with plastic to avoid humidity loss. The repaired portion of the beam had a length of 1.1 m.

4. Results

4.1 Cracking and visual damage

Damage on specimens at different stages are shown in Figs. 6 to 8. Drift ratios, corresponding to these figures are 1, 2 and 3%, respectively. Note that specimen C-1/CFRP is not presented but it is discussed in the following section instead.

Specimens C-1 and C-2 exhibited most damage in the beams, over a length of approximately one beam depth. Specimen C-1 experienced the most severe damage by the end of the tests. At drifts to 1%, joints had experienced minor damage (Figs. 6a and 6b). At 2% drift ratio, damage increased in the joint region (Figs. 7a and 7b). At 3% drift, the beams were considerably damaged. Note that no new cracks were formed at the joints, as can be observed in Figs. 8a and 8b. Concrete crushing and spalling was observed on specimens C-1, C-2, and C-2/SFRM during the final stages of the test.

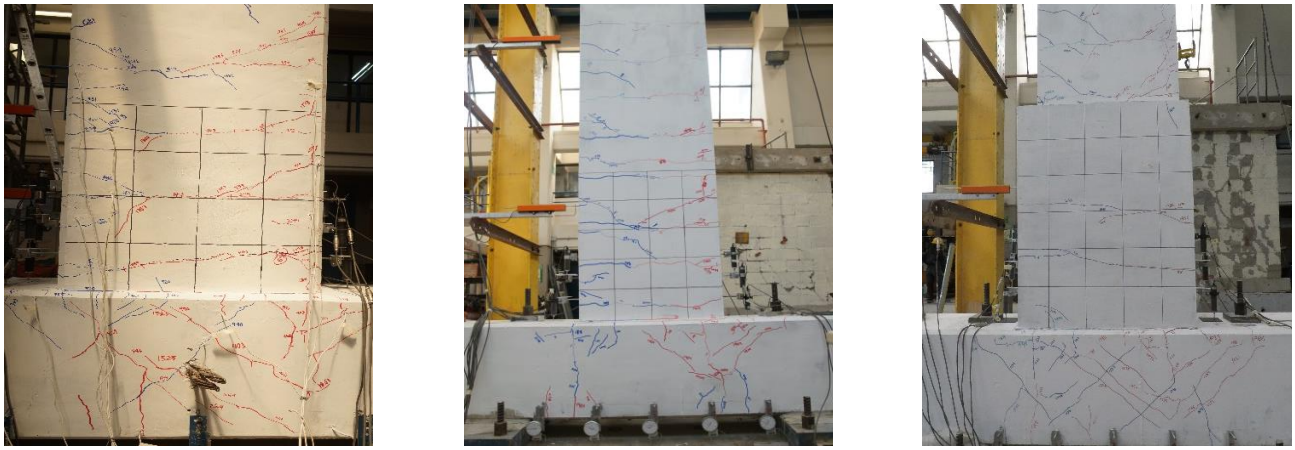

a) C-1 b) C-2 c) C-2/SFRM

Fig. 6 – Damage on specimens at 1% drift ratio

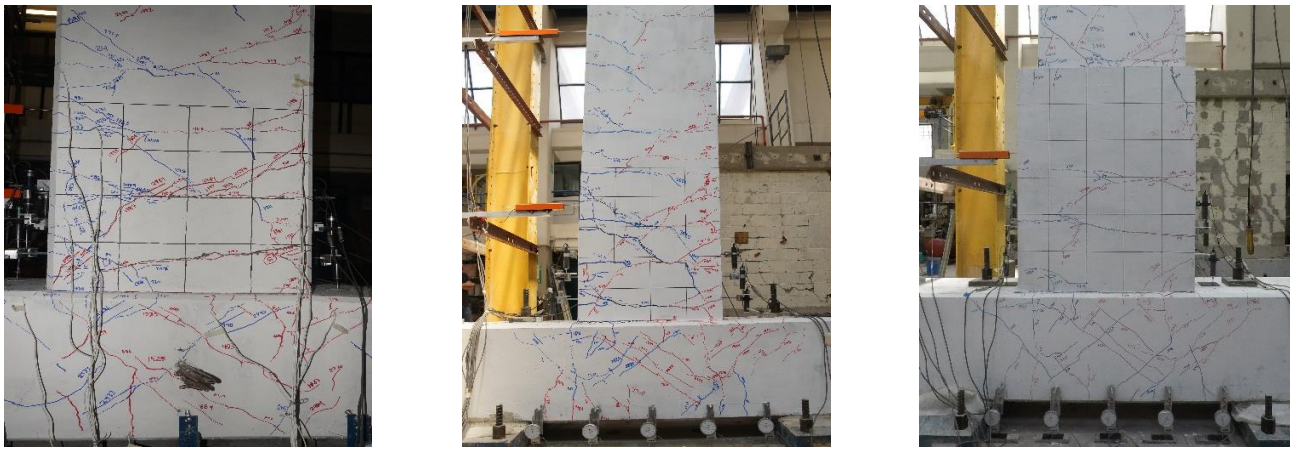

a) C-1 b) C-2 c) C-2/SFRM

Fig. 7 – Damage on specimens at 2% drift ratio

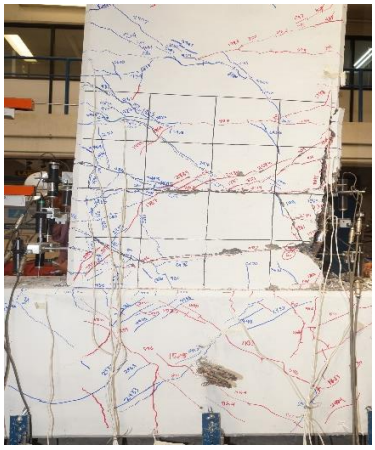
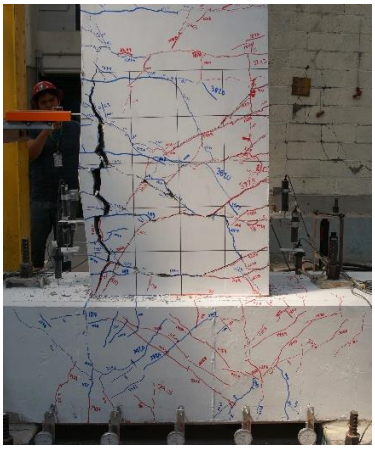
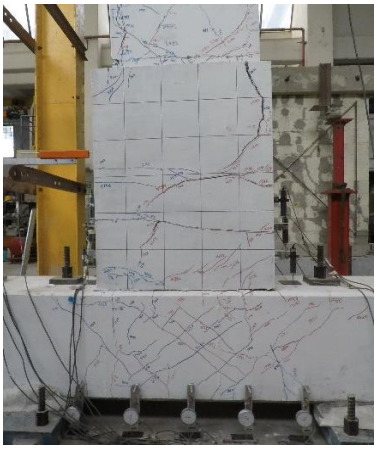

a) C-1 b) C-2 c) C-2/SFRM

Fig. 8 – Damage on specimens at 3% drift ratio

Specimen C-2/SFRM exhibited cracking in the joint at the beginning of the test and only minor damage on the SFRM jacket (see Figs. 6c and 7c). After that, damage was concentrated on the original beam section away from the column where the jacket ended (Fig. 8c). During the test, loud cracking sounds could be heard. This noises are credited to the debonding of the existing concrete and the SFRM.

4.2 Damage on specimen C-1/CFRP

Visual inspection of specimen C-1/CFRP showed that most damage was concentrated at the beam-column interface (Fig. 9a) and at the CFRP sheet ends (Fig. 9b). The longitudinal CFRP sheets contributed to this phenomenon, creating a plastic hinge relocation effect, which may be a desirable behavior for beam-column connections subjected to seismic loads. However, top and bottom cover concrete of the beam was pulled out by these sheets (Fig. 9b), thus it is recommended that they are not extended beyond the transverse sheets. Further, the CFRP sheets placed on the column proved to be unnecessary due to the beam longitudinal fiber breaking at the beam-column interface shortly after the test started (Fig. 9c).

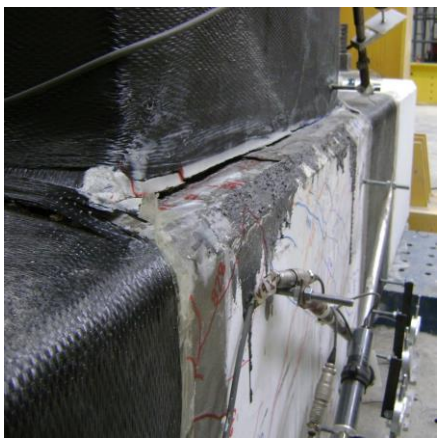

a) Beam-column interface b) Damage on beam c) Breaking of fiber

Fig. 9 – Damage on specimen C-1/CFRP

4.3 Load-drift ratio curves

Load-drift ratio curves of the specimens and their respective envelopes (in red) are shown in Fig. 10. Envelopes were obtained from the hysteresis curves, at each level of deformation, with the maximum load value for each set of cycles. The lateral drift ratio was defined as the ratio between the displacement at the loading point and the beam height.

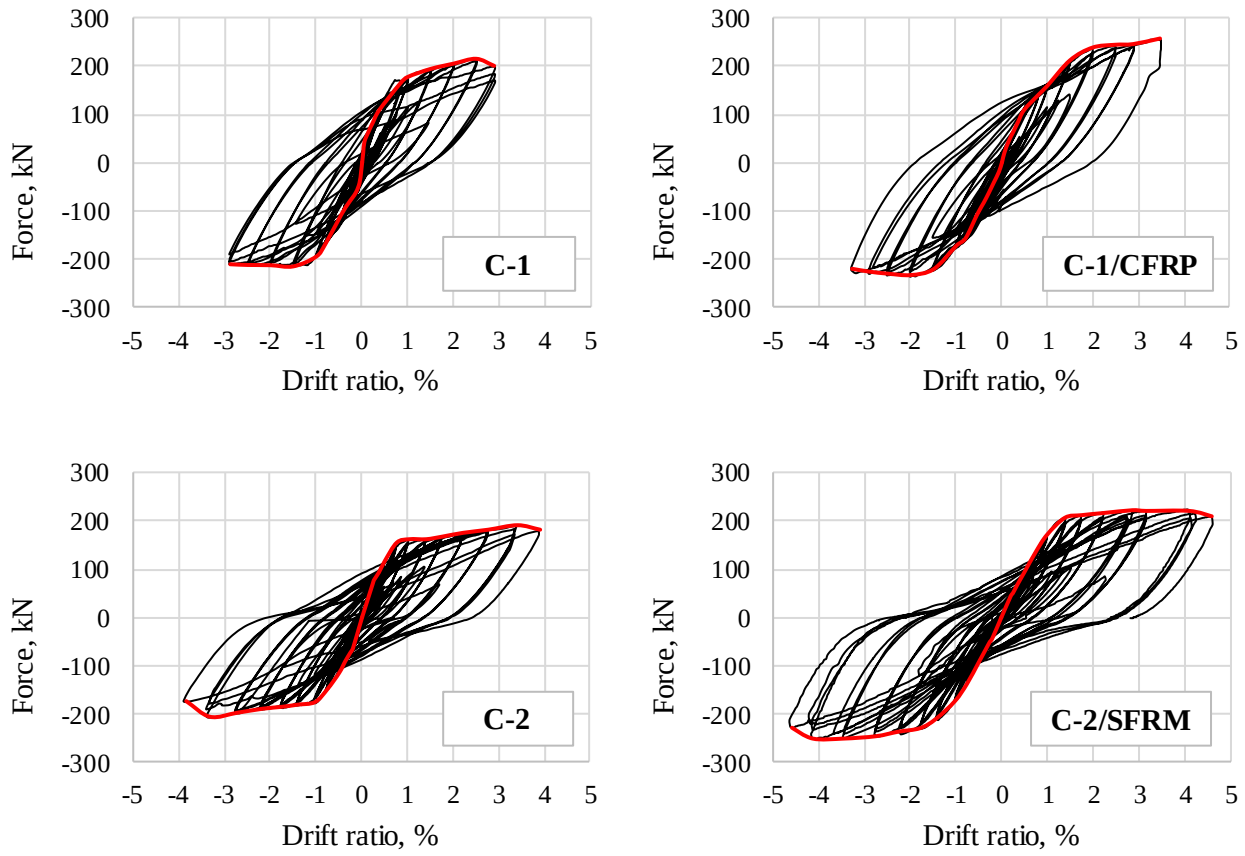

Fig. 10 – Load-drift ratio curves

Specimens exhibited adequate hysteretic behavior. After yielding, load-carrying capacities were increased, except for specimen C-2/SFRM, whose strength was maintained almost constant up to the final stages of the test. Tests were concluded prematurely due to the specimens displacing out of their plane after undergoing significant damage. As can be observed, the specimens were able to reach drift demands between 3 and 4.5%.

The load-drift ratio curves of all specimens are compared in Fig. 11. A comparison of the envelopes is also presented. As can be seen, specimens C-1 and C-2 were able to recover and, even, exceed their original load-carrying and deformation capacities after rehabilitation. Additionally, the effects of using different loading protocols can be observed. For example, specimen C-2, compared to specimen C-1, presented slightly smaller strength and stiffness. It was, however, able to be taken to drift ratios approximately 25% higher.

The load-carrying and deformation capacities of specimens are shown in Table 2. Load and deformation parameters were obtained with the component equivalency methodology from FEMA P-795 [13]. Ultimate deformation, Δ_U, is that corresponding to an 80% of the maximum load, F_{max}. However, the net maximum displacement was considered as the ultimate displacement as none of the specimens' peak load dropped 20%. Initial stiffness, K_i, is based on the force and deformation at $0.4F_{max}$. The effective yield deformation, Δ_y, and the effective ductility capacity, μ, were obtained as F_{max} / K_i and Δ_U / Δ_y, respectively.

Repaired specimens reached higher peak loads and effective yield deformation values than their original counterparts. In contrast, initial stiffness of the rehabilitated specimens was lower due to damage carried over from the first test, in addition to only the beam being rehabilitated. Specimens C-1/CFRP and C2/SFRM had, respectively, 23 and 31% less initial stiffness than the original specimens. Similarly, effective ductility capacity was greater for specimens C-1 and C-2, as these yielded at smaller displacements. It can be

observed that the load carrying capacity of the specimens was increased, as well as their effective yield deformation. Ultimate loads for specimens C-1 and C-2, after rehabilitation, were increased by 15 and 20%, respectively. However, ductility ratios were decreased. In terms of ultimate deformation, the rehabilitated specimens could be taken to larger deformation levels. Original and rehabilitated specimens yielded on average at 0.7 and 1.1% drift ratio, respectively.

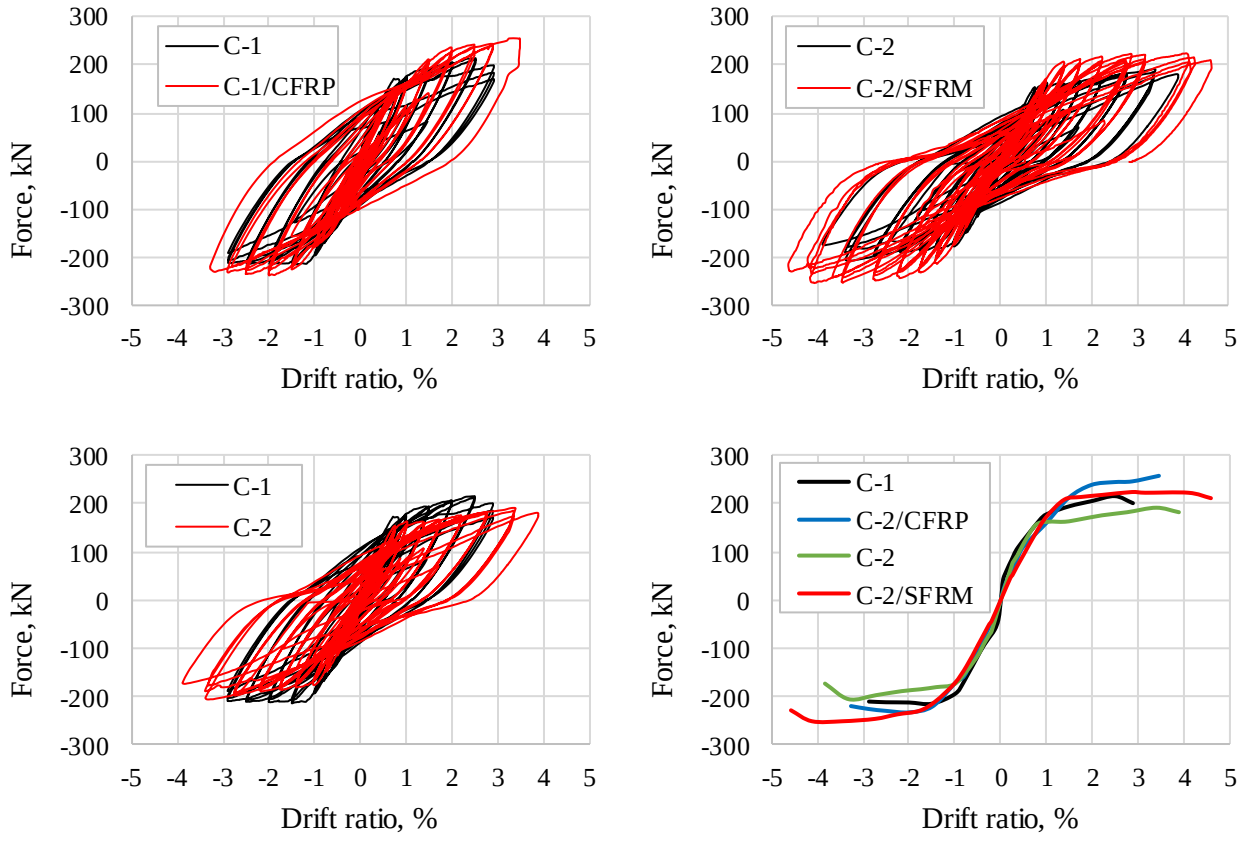

Fig. 11 – Comparisons of load-drift ratio curves

Table 2 – Load-carrying and deformation capacity of specimens

Specimen	Direction	F_{max}, kN	Δ_U, mm	K_i, kN/mm	Δ_y, mm	μ
C-1	Positive	215	145	6.1	35.0	4.1
	Negative	214	144	5.4	40.0	3.6
C-1/CFRP	Positive	256	174	4.7	55.0	3.2
	Negative	235	164	4.1	57.5	2.9
C-2	Positive	191	194	5.5	35.0	5.6
	Negative	207	192	5.2	40.0	4.8
C-2/SFRM	Positive	224	230	3.8	58.5	3.9
	Negative	253	229	3.7	67.5	3.4

4.4 Shear deformation

Joint shear deformations, before and after rehabilitation of the specimens, was studied in order to evaluate the adequacy of rehabilitating the beam only. It was expected that the strengthening of the beam would

increase the force and displacement demands on the joint. As a result, joint shear deformations were expected to increase. Joint shear deformation was obtained using Eq. 1:

$$\Delta_s = \frac{D_6 - D_5}{2\sin\theta} \tag{1}$$

where D_6 and D_5 are the measured displacements of the two diagonal LVDTs on the joint, shown in Fig. 3, and θ is the angle of inclination with respect to the horizontal axis (45°).

Joint shear deformation versus the applied force for all specimens is shown in Fig. 11. It can be seen that, after rehabilitation, shear deformation was increased for both specimens C-1/CFRP and C-2/SFRM, although it was minimal for specimen C-1 (less than 2 mm). In this case, most damage was concentrated at the column interface and on the top and bottom region of the beam where the CFRP sheets started and ended, creating a plastic hinge relocation effect which contributed to a good behavior of the joint. In contrast, shear deformation on specimen C-2 was significantly increased (up to 10 mm in the positive direction) as the SFRM jacket left the joint as the next weakest link in the system. In any case, regardless, strengthening of the joint should be considered.

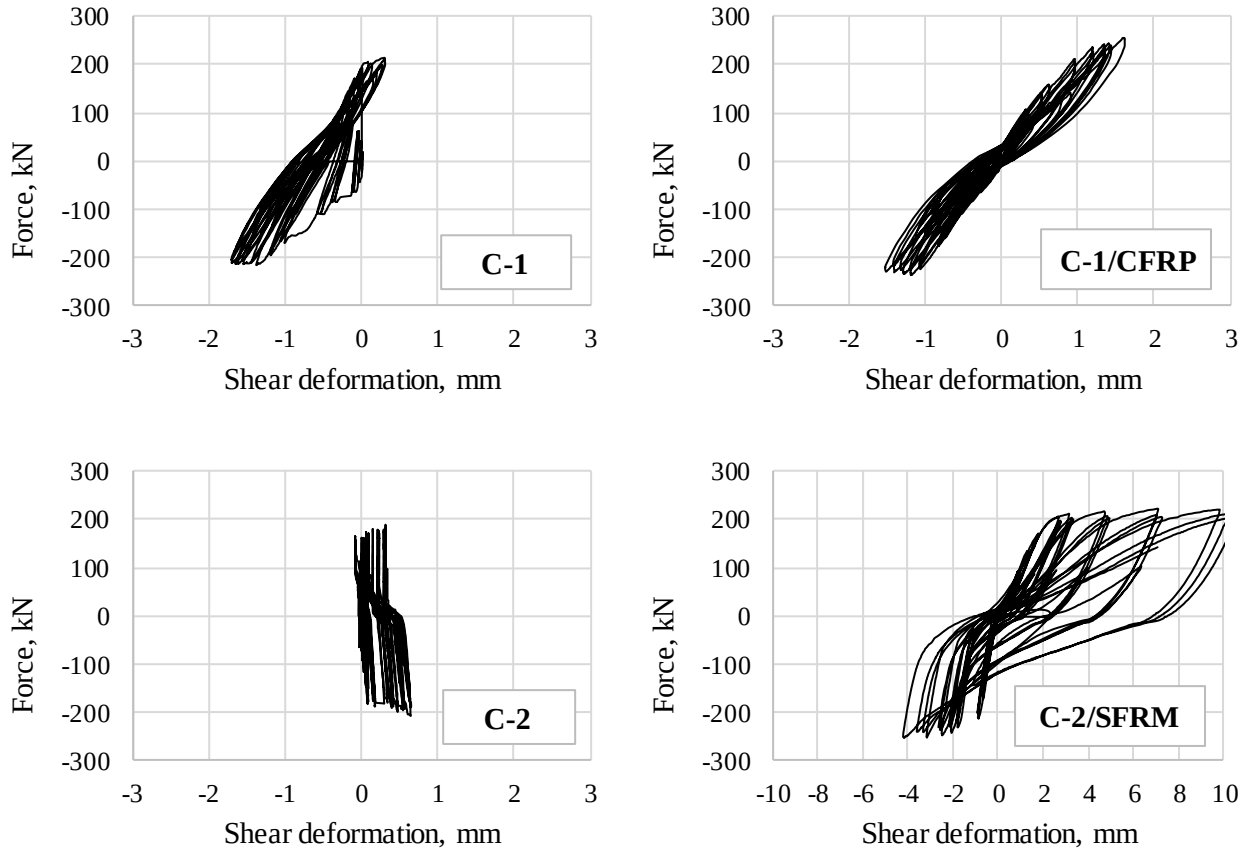

Fig. 11 – Joint shear deformation

5. Conclusions

Two full-scale monolithic RC beam-column joints were tested under different loading protocols and retested after their rehabilitation using two different techniques: externally bonded carbon fiber reinforced polymer

for one specimen and steel fiber reinforced mortar for the other. Performance of specimens, before and after rehabilitation, was presented and discussed in terms of visual damage and cracking; strength and drift capacity; and shear deformation. Based on the experimental results, the following conclusions can be made:

1. Externally bonded CFRP sheets and SFRM jacketing were considered appropriate methods for the rehabilitation of concrete beams with low transverse reinforcement that have been heavily damaged due to seismic loading. In both cases, original load-carrying and deformation capacities were recovered and slightly exceeded. This is a desirable attribute when rehabilitating damaged buildings because their overall behavior is not affected significantly. However, section enlargement and added weight of the SFRM jacket should be considered.
2. Increased joint shear cracking was a concern beforehand. Specimen C-1 behaved adequately, presenting minor shear deformation before and after rehabilitation. The relocation effect of the plastic hinge, primarily due to the longitudinal fiber sheets, concentrated the inelastic deformations on the beam and contributed to a good behavior of the joint. In contrast, shear deformation was significantly increased in specimen C-2/SFRM due to the strengthening of the beam leaving the joint as the next weakest link in the system. In any case, strengthening of the joint should be considered to avoid unexpected failures. The weak beam-strong column mechanism should also be warranted.
3. While the results show that CFRP and SFRM jacketing of heavily damaged beams are adequate rehabilitation methods, the number of specimens is insufficient and more research is needed in order to better understand their limitations and develop adequate guidelines for their use.

6. Acknowledgements

The financial support of the Mexican National Council for Science and Technology, CONACyT, through the FORDECyT 297246 project, is gratefully acknowledged. The first author would like to express gratitude for the scholarship provided by CONACyT to conduct his doctoral studies. Acknowledgement is expressed to, ITISA for donating the tested specimens; Sika Mexico for conducting the rehabilitation of specimen C-1; Granding International for conducting the rehabilitation of specimen C-2; and Mexico's National Disaster Prevention Center (CENAPRED) for providing the facilities to conduct the experiment.

7. References

[1] Engindeniz M, Kahn LF, Zureick AH (2005): Repair and strengthening of reinforced concrete beam-column joints: state of the art. *ACI Structural Journal*, Vol. 102, No. 2.

[2] ACI Committee 440 (2017): Guide for the design and construction of externally bonded FRP systems for strengthening concrete structures (ACI 440.2R-17). *American Concrete Institute*, Farmington Hills, Mich.

[3] Issa CA, AbouJouadeh A (2004): Carbon fiber reinforced polymer strengthening of reinforced concrete beams: experimental study. *Journal of Architectural Engineering*, ASCE.

[4] Bonfiglioli B, Pascale G, de Mingo SM (2004): Dynamic testing of reinforced concrete beams damaged and repaired with fiber reinforced polymer sheets. *Journal of Materials in Civil Engineering*, ASCE, 16, 400-406.

[5] Shahawy M, Beitelman TE (1999): Static and fatigue performance of RC beams strengthened with CFRP laminates. *Journal of Structural Engineering*, 125 (6), 613-621.

[6] Ghobarah A, Ghorbel MN, Chidiac SE (2002): Upgrading torsional resistance in reinforced concrete beams using fiber-reinforced polymer. *Journal of Composites for Construction*, 6(4), 257-263.

[7] Carrillo J, Alcocer SM (2016): Muros de concreto reforzado con fibras de acero Desempeño sismo-resistente basado en ensayos en mesa vibratoria. *ECOE Ediciones*, México.

[8] ACI Committee 544 (1996): Report on fiber reinforced concrete (ACI 544.1R-96). *American Concrete Institute*, Farmington Hills, Mich.

[9] Carrillo J, William A, González G (2013): Correlaciones entre las propiedades mecánicas del concreto reforzado con fibras de acero. *Ingeniería Investigación y Tecnología*, Vol. 14, 435-450.

[10] Ávila O, Carrillo J, Alcocer SM (2011): Rehabilitación de muros de concreto usando CRFA: ensayos en mesa vibradora. *Concreto y Cemento Investigación y Desarrollo*, Vol. 2, No. 2, 2011.

[11] RCDF (2017). Mexico City building code and its complementary specifications. Mexico City, Mexico.

[12] ACI Committee 374 (2013): Guide for testing reinforced concrete structural elements under slowly applied simulated seismic loads (ACI 374.2R-13). *American Concrete Institute*, Farmington Hills, Mich.

[13] FEMA P-795 (2011). Quantification of building seismic performance factors: component equivalency methodology. *Federal Emergency Management Agency*. Washington, DC.

